Environ. Sci. Technol. **2005**, *39,* 1658−1665

Nonmonotonic Variations in Deposition Rate Coefficients of Microspheres in Porous Media under Unfavorable Deposition Conditions

XIQING LI AND WILLIAM P. JOHNSON*

Department of Geology & Geophysics, University of Utah, Salt Lake City, Utah 84112-0111

The transport of carboxylate-modified polystyrene latex microspheres was examined in packed quartz sand under a variety of environmentally relevant ionic strength and flow conditions. The retained concentrations of microspheres in the sediment increased first, and then decreased with transport distance, indicating that the deposition rate coefficient changed nonmonotonically over the transport distance. This finding demonstrates the ubiquity of spatial variation in deposition rate coefficients under unfavorable deposition conditions, and in addition indicates that the previously recognized monotonic decrease with transport distance is not the sole form of spatial variations in deposition rate coefficients. In contrast, the deposition rate coefficients of similarly sized microspheres with different surface group densities were shown to decrease monotonically with transport distance in the same porous media, indicating that the form of spatial variation in deposition rate coefficient is highly sensitive to system conditions. The ubiquity and sensitivity of the spatial variation of deposition rate coefficients indicate that current practices that utilize log-linear extrapolation of discreet measurements of colloid attenuation to determine colloid removal with distance from source are not valid (for both biological and nonbiological colloids). The retained colloid profiles hold the promise to reveal processes governing colloid deposition under unfavorable conditions that are yet to be identified.

Introduction

Colloid transport experiments in porous media have mainly focused on the determination of concentrations in the effluent (generation of breakthrough−elution curves) due to ease of analysis relative to determination of retained colloid concentrations. Investigations that have examined the retained colloid concentrations have shown that retained colloid concentrations decrease with distance from source at a rate much greater than is consistent with a constant deposition rate coefficient. A constant deposition rate coefficient is implicit in "clean-bed" filtration theory (*1*), which results in prediction of log-linear decreases in retained colloid concentrations with transport distance. Deviation of the retained profile from expectations was first demonstrated in the biological colloid transport literature a decade ago (*2*) and has been corroborated by numerous subsequent transport studies of bacteria in the laboratory (*3*−*5*), bacteria in the field (*6*−*8*), as well as viruses in the laboratory (*9*, *10*) and the field (*11*−*14*). To describe the retained profiles, bimodal (*3*−*5*, *15*), power-law (*9*, *10*), as well as log-normal (*16*) distributions of the deposition rate coefficients among the cell population have been invoked.

Recently, Li et al. (*17*) showed apparent decreases in deposition rate coefficients of nonbiological colloids with increased distance of transport in columns packed with glass beads. The profiles of retained carboxylated microspheres in glass beads were shown to be consistent with a log-normal distribution of deposition rate coefficients among the microsphere population. Furthermore, Li et al. (*17*) demonstrated that log-linear retained profiles were obtained under favorable deposition conditions (where colloid-grain surface repulsion is absent), and that deviations from this behavior increased with increasingly unfavorable deposition conditions (where colloid-grain surface repulsion dominates). It therefore appears that decreases in apparent deposition rate coefficients with transport distance are general to both biological and nonbiological colloids and are the norm under environmental conditions where interactions are generally unfavorable.

Reported deviations from log-linear retained profiles have to date mainly involved decreases in deposition rate coefficient with increasing transport distance (as described above). However, other forms of deviation from log-linear retained profiles have occasionally been reported. For example, Bolster et al. (*5*) observed that under a single experimental condition, retained concentrations of bacteria increased slightly from the column inlet before decreasing toward the outlet. Harter et al. (*18*) observed that under some conditions the maximum concentrations of retained *Cryptosporidium Parvum* oocysts were located down-gradient of, rather than at, the inlet of the column. Redman et al. (*9*, *10*) reported that the deposition rate coefficients of recombinant Norwalk viruses in quartz sand reached maximum values down-gradient of the column inlet. The two former publications did not attempt to explain these observations, whereas the two latter publications attributed the reduced virus deposition at the inlet of the column to masking of favorable attachment sites by adsorbed organic matter that was originally present in suspending solution (groundwater or wastewater). This implies that the observed nonmonotonic variations in retained concentrations with distance resulted from effects of constituents in the system other than the colloids or the porous media, and do not represent processes inherent in filtration under unfavorable conditions.

The objective of this paper is to demonstrate that nonmonotonic spatial variations in retained colloid concentrations are obtained under unfavorable conditions in simple systems (e.g., lacking organic matter). This finding demonstrates the ubiquity of spatial variations in deposition rate coefficients of colloids under unfavorable deposition conditions and indicates that the form of spatial variation is highly sensitive to the system conditions. The generality and sensitivity of the spatial variation of deposition rate coefficients invalidate practices (used for both biological and nonbiological colloids) that log-linearly extrapolate colloid removal with distance from source.

Methods

Experimental Methods. The microspheres used in column experiments were spherical fluorescent carboxylate-modified polystyrene latex microspheres of two similar sizes but different surface properties (diameters of 1.1 and 1.0 μm,

* Corresponding author phone: (801)581-5033, fax: (801)581-7065; e-mail: wjohnson@mines.utah.edu.

10.1021/es048963b CCC: $30.25
Published on Web 01/26/2005

TABLE 1. Column Experiment Conditions, Mass Balances, and Model Parameters for Simulations Using the Particle-Tracking Model[a]

size (μm)	IS (M)	buffer	vel	N	% rec	% sed	k_f (h^{-1})	k_r (h^{-1})	f_{ir}
1.1	0.001*	MOPS	4	2	106.5	5.6	0.053	0.26	0.80
1.1	0.003	MOPS	4	1	105.0	22.4	0.22	0.24	0.961
1.1	0.006	MOPS	4	2	102.1	62.7	0.83	0.20	0.980
1.1	0.02	MOPS	4	2	94.6	93.0	3.53	0.20	0.996
1.1	0.006	MOPS	2	2	86.4	81.0	1.2	0.10	0.995
1.1	0.006	MOPS	8	2	100.1	34.2	0.72	0.38	0.980
1.1	0.003	$NaHCO_3$	4	2	88.5	60.7	1.03	0.20	0.95
1.1	0.006	$NaHCO_3$	4	2	92.4	78.7	1.65	0.21	0.968
1.1	0.02	$NaHCO_3$	4	2	94.3	94.1	5.32	0.20	0.991
1.0	0.001	MOPS	8	2	94.8	5.9	0.16	0.45	0.65
1.0	0.001	$NaHCO_3$	8	2	103.8	20.2	0.47	0.55	0.75
0.93	0.001	MOPS	4	1	91.2	91.2	8.5	0.0	1.0
0.93	0.001	MOPS	8	2	105.9	105.7	10.8	0.1	0.988

[a] "Size" refers to diameter of microspheres. "IS" indicates ionic strength (M). "Vel" indicates pore water velocity (m day^{-1}). "*N*" refers to the number of replicates. "% Rec" refers to average percent recovery for the experimental condition. "% Sed" refers to average percent of microspheres retained on sediment at the end of the experiment. * refers to conditions for which experiment data were not shown.

and surface carboxylate group densities of 7.9×10^7 and 4.9×10^6 per sphere, respectively). The microsphere stock suspensions (Molecular Probes, Inc., Eugene, OR) were used as received with a particle concentration of 2.7×10^{10} mL^{-1} (1.1 μm, high surface group density) and of 3.6×10^{10} mL^{-1} (1.0 μm, low surface group density). Prior to injection, an aliquot of stock suspensions was diluted to achieve an influent concentration (C_o) of 3.5×10^6 ±15% particles mL^{-1} in salt solutions with desired ionic strengths.

The porous media used for column experiments was 30−40 mesh (417−600 μm) quartz sand (Unimin Corp., New Canaan, CT). The quartz sand was cleaned by soaking in concentrated HCl for at least 24 h, followed by repeated rinsing with ultrapure water (Millipore Corp. Bedford, MA), drying at 105 °C, and baking overnight at 850 °C. The cleaned sand was stored under argon gas. Prior to the column experiments, the sand was rehydrated by boiling in pure water for at least 1 h. The cylindrical Plexiglass columns (20 cm in length and 3.81 cm in inner diameter) were dry-packed after the rehydrated quartz sand was dried at 105 °C and cooled. The porosity of the packed quartz sand was 0.36. The mass of packed quartz sand in each column differed by no more than 2 g (less than 0.6% of the total sediment mass).

The packed columns were purged with CO_2 for at least 15 min and then were preequilibrated with about 10 pore volumes of microsphere-free salt solution at pH of 6.92, buffered by NaOH/MOPS(3-[*N*-morpholino]propanesulfonic acid). One pore volume was equal to 81.5 mL at a porosity of 0.36. Following preequilibration, the effluent pH consistently differed by no more than 0.02 units from that of the influent. After preequilibration, 3 pore volumes of microsphere suspension was injected, followed by 7 pore volumes of elution with buffered salt solution (without microspheres) at the same ionic strength and pH. The suspensions and solutions were injected in up-flow mode using a syringe pump (Harvard Apparatus Inc., Holliston, MA). During injection, the microsphere suspension reservoirs were sonicated for 1 min each hour to minimize aggregation. For the microspheres with high surface group density (1.1 μm), the transport experiments were carried out at four ionic strengths, 0.001, 0.003, 0.006, and 0.02 M. The flow rate was varied to produce pore water velocities of 2, 4, and 8 m day^{-1}. A comparison experiment was run using the microspheres with low surface group density (1.0 μm) at the 0.001 M ionic strength and 8 m day^{-1} flow rate condition. The experimental conditions are summarized in Table 1. More details of the column experiment procedure were provided in a previous paper (*17*).

Column effluent samples were collected in 5 mL polystyrene tubes with a fraction collector (CF-1, Spectrum Chromatography, Houston, TX). Following the experiment, the sediment was dissected into 10 2-cm-long segments, as the sediment was released from the column under gravity. Retained colloids were recovered by placing sediment segments (2 cm) into specified volumes of Milli-Q water and sonicating for 1 min, followed by manual vigorous shaking for a few seconds. These specified volumes were 100 mL for the first three segments at the column inlet, and 25 mL for all subsequent segments.

Aqueous effluent samples, and supernatant samples from recovery of retained microspheres, were analyzed using flow cytometry (BD FACScan, Becton Dickinson & Co., Franklin Lakes, NJ). The samples were run using a flow rate of 12 μL min^{-1} at an excitation wavelength of 488 nm and were counted for 1 min. Conversion of "event" counts on the flow cytometer into microsphere concentrations was made using a calibration curve based on serial dilutions of microsphere suspensions of known concentration. The R^2 values of the log−log calibration curves were consistently greater than 0.99.

The area under the breakthrough−elution curve was integrated to yield the percentage of microspheres exiting the column. The percent of injected microspheres recovered from the sediment was determined by summing the number of microspheres recovered from all segments of the sediment and dividing by the total number injected. The overall recovery (mass balance) of microspheres was determined by summing the percentages of microspheres that exited and that were retained in the column.

Numerical Simulations. The transport of the microspheres was modeled using an advection-dispersion equation that includes deposition from, and re-entrainment to, the aqueous phase:

$$\frac{\partial C}{\partial t} = -v\frac{\partial C}{\partial x} + D\frac{\partial^2 C}{\partial x^2} - k_f C + \frac{\rho_b}{\theta} k_r S_r \qquad (1)$$

where C is the microsphere concentration in aqueous phase (particles per unit volume of fluid), t is the travel time, x is the travel distance, v is the flow velocity, D is the dispersion coefficient of the colloid particles, θ is the porosity, ρ is the bulk density of sediment, and k_f and k_r are rate coefficients of microsphere deposition to and re-entrainment from solid phase, respectively. S_r is the reversibly retained microsphere concentration on the solid phase (particles per unit mass of sediment) and can be further expressed as

$$S_r = S(1 - f_{ir}) \qquad (2)$$

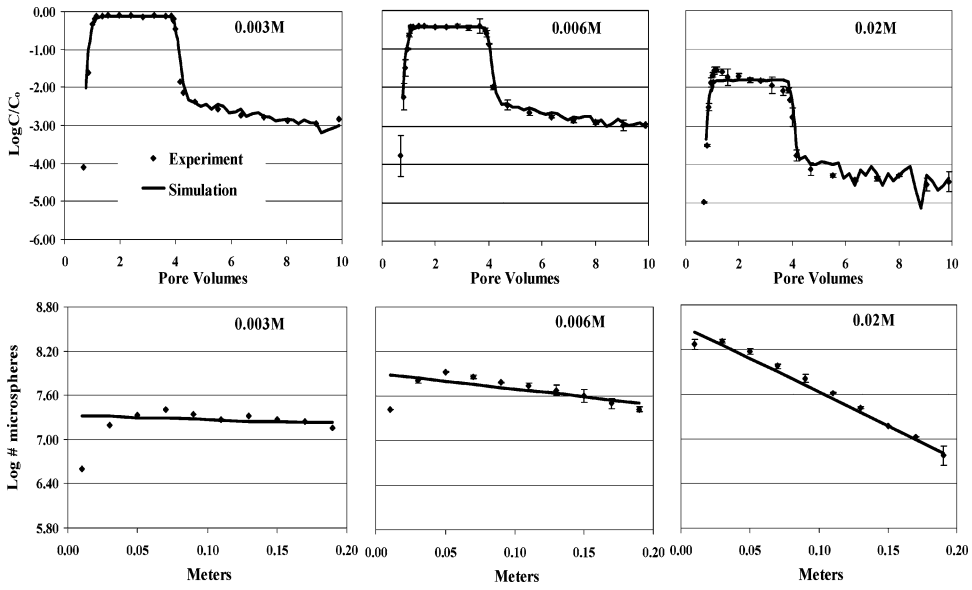

FIGURE 1. Effluent breakthrough−elution curves (top) and retained profiles (bottom) of the 1.1-μm microspheres at different ionic strengths using MOPS buffer (flow rate = 4 m day^{-1}). Error bars represent standard deviations in results from replicate experiments ($n \geq 2$). Solid lines represent simulations using the particle tracking model with a single deposition rate coefficient. C and C_o are the effluent and influent concentrations, respectively. "Log # of microspheres" refers to the number (in log scale) of microspheres retained in each sediment segment.

where S is the total deposited concentration and f_{ir} is the fraction of irreversible deposition.

A one-dimensional discrete random-walk particle-tracking model was used to simulate microsphere transport (eq 1) in column experiments. In the particle model, deposition from the aqueous phase is represented in a discrete form by assigning a probability of deposition to each numerical particle in each time step. The probability of deposition in any time step is given by the deposition rate coefficient (k_f) multiplied by the time step. An analogous procedure is used to represent the re-entrainment process using a re-entrainment rate coefficient (k_r) that is applied to the reversibly deposited population of colloids. The particle model also allows for the simulation of partially irreversible deposition via a fraction of irreversible deposition (f_{ir}) that is specified by the user. At each time step and for each numerical particle, a uniform pseudorandom number between 0 and 1 is generated and compared to the probability of deposition (or re-entrainment). If the random number is less than the assigned probability, then deposition (or re-entrainment) occurs. Likewise, a uniform pseudo-random number is generated upon deposition and compared to f_{ir}. If the random number is less than f_{ir}, then the particle is assigned a flag that designates it as irreversibly deposited and it will not be subsequently considered for re-entrainment.

Results

Mass Balance. Mass recoveries (total from effluent and sediment) were all between 86% and 107% (Table 1), equivalent to those observed with glass beads (*17*). The excellent mass recoveries required only minor adjustments of effluent and retained concentrations of microspheres to yield 100% mass balances for simulations. Hence, these adjustments would not affect the analysis presented below.

Effluent Curves and Retained Profiles. Results for the 1.1-μm microspheres at different ionic strengths and flow rates are shown in Figures 1 and 2, respectively. The effluent breakthrough−elution curves (Figures 1 and 2, top) represent the normalized effluent concentration, C/C_o, during injection and elution. The retained profiles (Figures 1 and 2, bottom) represent the number of retained colloids in sediment as a function of transport distance. Error bars in the effluent breakthrough−elution curves and the retained profiles represent standard deviations from replicate experiments ($n \geq 2$). The magnitude of the steady-state breakthrough plateau decreased with increasing ionic strength and decreasing flow rate (Figures 1 and 2, top). At two experimental conditions (0.02 M, 4 m day^{-1} and 0.006 M, 2 m day^{-1}), the breakthrough plateau (2−4 pore volumes) showed a slight but continuous decline, indicating a temporal increase in the deposition rate during the course of injection (e.g., a ripening effect). These experimental conditions were simulated with a temporally constant deposition rate coefficient that reflected the average deposition rate coefficient during the experiment.

The magnitude of the retained microsphere profiles increased with increasing ionic strength and decreasing flow rate (Figures 1 and 2, bottom), in correspondence with the effluent curves. The same trends were previously described for microsphere transport in the glass beads (*17*).

The shapes of the retained profiles in quartz contrasted strongly with those previously observed in the glass beads (*17*). In the quartz sediment, the numbers of retained microspheres first increased, and then decreased, with distance of transport. In contrast, in the glass beads the numbers of retained microspheres decreased monotonically, more rapidly than what would be predicted based on a spatially constant first-order deposition rate coefficient (*17*).

The maximum retained concentrations were located increasingly down-gradient with decreasing ionic strength (Figure 1, bottom). The distance from the inlet decreased from 7 to 3 cm over the ionic strength range from 0.003 to 0.02 M. In contrast, the maximum retained concentrations shifted negligibly down-gradient in response to increased flow rate (Figure 2, bottom). These results indicate that the down-gradient location of the maximum retained concentration was governed by grain−microsphere interaction and not by hydrodynamic forces at the grain surfaces. The opposite conclusion was drawn in recent work examining transport of an adhesion-deficient soil bacterial strain (*19*), where the maximum retained concentration was increasingly shifted down-gradient with increasing flow rate and increasing elution time, strongly implicating bacterial detachment as a major governor of the distribution of retained bacteria in that porous media (glass beads).

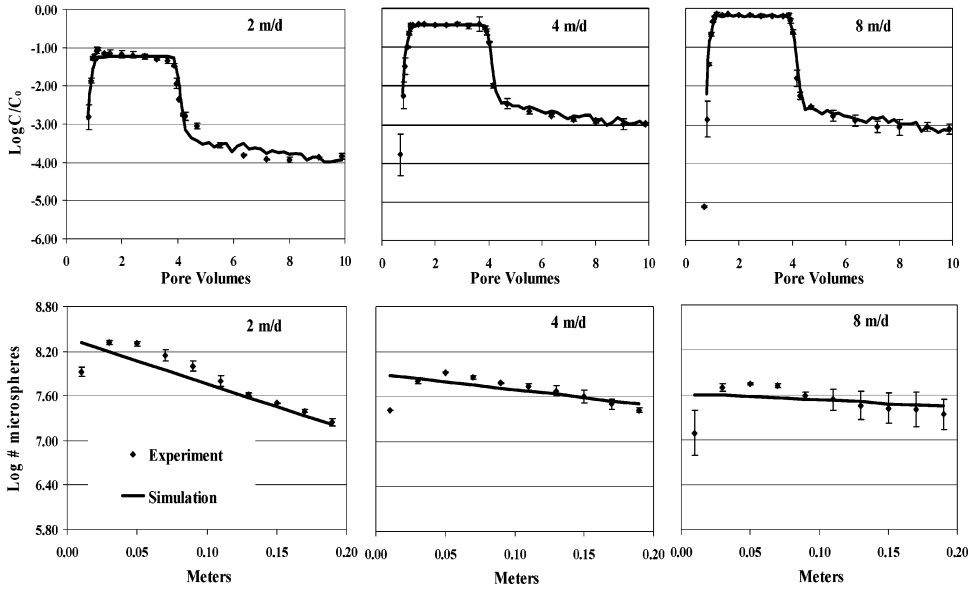

FIGURE 2. Effluent breakthrough−elution curves (top) and retained profiles (bottom) of the 1.1-μm microspheres at different flow rates using MOPS buffer (ionic strength = 0.006 M). Error bars represent standard deviations in results from replicate experiments ($n \geq 2$). Solid lines represent simulations using the particle tracking model with a single deposition rate coefficient.

Deviation of Retained Profiles from Expectations. The particle transport model was able to simulate well the effluent curves (Figures 1 and 2, top). Regular trends were observed in the parameters derived from simulations (Table 1), as was observed in the glass beads (*17*). These trends will be discussed in a separate paper that will examine the relationship of these trends to interaction forces and hydrodynamic drag (*20*). The retained profiles, however, could not be fit by the simulations (Figures 1 and 2, bottom) using a spatially constant deposition rate coefficient (which yielded log-linear decreases in retained colloid concentrations with transport distance). In contrast to the results shown above for the 1.1-μm microspheres, the retained concentrations of the 1.0-μm microspheres (low surface group density) in quartz sand (0.001 M ionic strength and 8 m day^{-1} flow rate) decreased monotonically and at a rate greater than that based on a spatially invariant deposition rate coefficient (Figure 3, left bottom), as observed for both the 1.1-μm and the 1.0-μm microspheres in glass beads (*17*), indicative of decreases in the deposition rate coefficient with transport distance. Because the major difference between the two sizes of microspheres is their surface group density, it is clear that surface property of microspheres (grain−microsphere interaction) plays an important role in determining the shape of the retained profile and the form of spatial variation of the deposition rate coefficients. This contrast demonstrates that the form of spatial variations of deposition rate coefficients is highly system-specific.

Extent of Re-entrainment of Retained Microspheres. It is possible that the observed increase-then-decrease in retained microsphere concentration was caused by substantial re-entrainment of retained microspheres yielding down-gradient movement of the center of retained mass. This process was observed in recent bacterial transport experiments (*19*). Convex-upward retained profiles, similar to those observed here, were generated in bacterial transport models that simulated substantial re-entrainment of retained colloids (*16*). To determine whether re-entrainment during elution was responsible for the apparent increase-then-decrease in deposition rate coefficient with transport distance, elution times were varied to determine whether the location of the center of mass of retained microspheres increased with increasing elution time (1.3, 7, 14, and 21 pore volumes). This experiment was run at an ionic strength

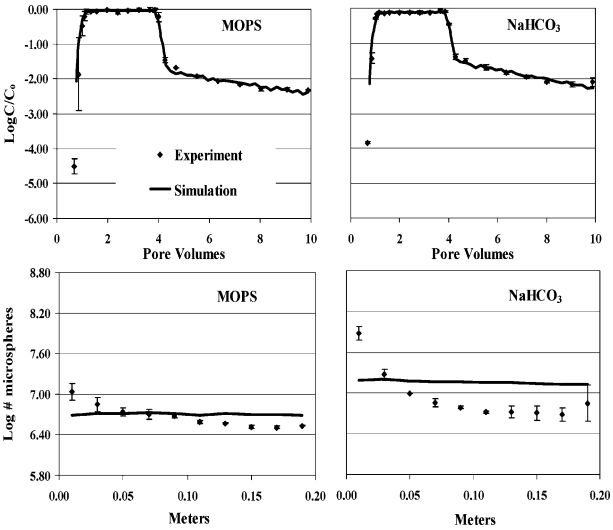

FIGURE 3. Effluent breakthrough−elution curves (top) and retained profiles (bottom) of the 1.0-μm microspheres (lower surface charge density), using MOPS (left) and $NaHCO_3$ (right) buffers (ionic strength = 0.001 M, flow rate = 8 m day^{-1}). Error bars represent standard deviations in results from replicate experiments ($n \geq 2$). Solid lines represent simulations using the particle tracking model with a single deposition rate coefficient.

of 0.006 M, and a flow rate of 8 m day^{-1} using the 1.1-μm microspheres. The breakthrough−elution curves were roughly equivalent for the series of columns corresponding to various elution times (Figure 4, top). The magnitude and the location of the center of mass of the retained microspheres were equivalent within experimental error for the various elution durations (Figure 4, bottom), indicating that re-entrainment of retained microspheres did not govern the observed increase-then-decrease in deposition rate coefficient with transport distance. The absence of substantial re-entrainment during elution is also evidenced by the low eluted concentrations following the breakthrough plateau, which yielded high fractions of irreversible deposition (f_{ir}) (greater than 0.96 for the 1.1-μm microspheres except at 0.001 M, Table 1). The extended tailing concentrations observed in Harter et al. (*18*) and Redman et al. (*9*, *10*) were lower or roughly equivalent to those observed here. Therefore, re-entrainment

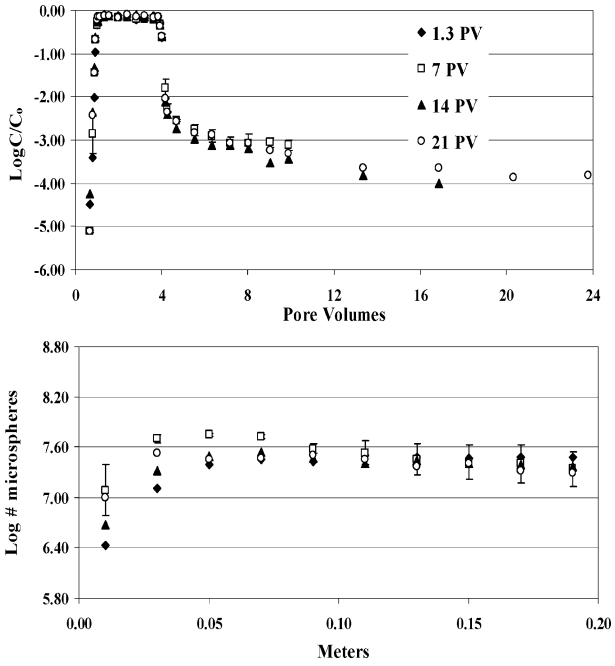

FIGURE 4. Effluent breakthrough−elution curves (top) and retained profiles (bottom) of the 1.1-μm microspheres for different elution times (ionic strength = 0.006 M, MOPS buffer, flow rate = 8 m day^{-1}).

during elution does not appear to be responsible for the observed down-gradient location of maximum retained concentrations in their studies.

Re-entrainment could be potentially enhanced preferentially during microsphere injection (1−3 pore volumes) as a result of increased hydrodynamic collision (*21*), because concentrations of mobile microspheres were much higher during injection than during elution. To examine whether the down-gradient location of the maximum retained microsphere concentrations was governed by hydrodynamic collision during injection, an experiment was run with low influent concentration (3.5×10^5 sphere/mL^{-1}, 1/10 of influent concentrations used in other experiments performed under unfavorable conditions). The 1.1-μm microspheres were run at a flow rate of 4 m day^{-1} and an ionic strength of 0.006 M. Approximately the same down-gradient location was observed for the maximum retained microsphere concentrations as with the higher influent concentration (3.5×10^6 sphere/mL^{-1}) under equivalent flow and ionic strength conditions (data not shown). Hydrodynamic collision therefore does not appear to be the source of observed nonmonotonic retained profiles.

Discussion

Potential Artifacts Yielding Distributed Deposition Rates. The possibility that distance-dependent changes in deposition rate coefficients might be caused by experimental artifacts was addressed in the previous paper (*17*). Potential artifacts discussed included pH change across the length of the column, sediment heterogeneity due to packing and grain migration during injection, as well as flow heterogeneity due to inadequate spreading of flow upon entry into column. All of these can be ruled out as artifacts leading to the observed nonmonotonic variations of removal rate coefficients with transport distance as follows: influent and effluent pH were virtually the same and constant throughout all experiments; log-linear decreases in retained microsphere concentrations with distance were observed under favorable conditions (shown below), which clearly precludes control by sediment and flow heterogeneities. As well, the possibility that contaminants in the stock microsphere suspension resulted in the observed nonmonotonic profiles was refuted by experiments performed following washing the stock microsphere suspensions three times in pure water (via centrifugation and resuspension).

Attractive microsphere−microsphere interaction and aggregation could potentially cause deviation of retained profiles from those predicted by "clean-bed" filtration theory. To avoid aggregation effects, the stock microsphere suspension was sonicated (1 min) every hour during injection. Because the deviation from log-linear retained profiles occurred at the column inlet, 1 h is sufficient time to represent possible degree of aggregation in the column. The stock suspension at 0.02 M ionic strength (highest) was examined 1 h after sonication using a grooved slide under a microscope. Only 3% doublets and negligible triplets were observed, in qualitative agreement with manufacturer's claim (98.6% percent singlets). The negligible aggregation relative to deposition (Table 1) indicates a lack of microsphere−microsphere attraction. This result agrees with the observed lack of temporal increase in the deposition rate during the experiments (constant breakthrough plateau). As well, it agrees with large energy barriers calculated for microsphere−microsphere interaction, 1.7×10^3, 1.5×10^3, and 1.1×10^3 kT, respectively, at the above ionic strengths (calculation described below).

The nonmonotonic changes of retained microsphere concentrations with transport distance are similar to those observed in other investigations by Harter et al. (*18*) and Redman et al. (*9*, *10*). The latter attributed their observed increase-then-decrease in retained virus concentrations with distance across the column to the adsorption of organic matter present in the suspending solution (groundwater and wastewater). Adsorbed organic matter near the column inlet was presumed to decrease colloid attachment via increased electrostatic repulsion between the colloids and the grain surfaces.

The possibility that the organic buffer (MOPS) adsorbed to the grain surfaces near the column inlet was tested in column experiments run at the same influent microsphere concentrations using $NaHCO_3$ (rather than MOPS) to adjust pH to 6.75 ± 0.05. The columns were preequilibrated with more than 30 pore volumes of microsphere-free solution. Throughout the injection and elution, influent and effluent pH differed by no more than 0.05 units for each experiment. At 0.003 and 0.006 M ionic strengths, the retained concentrations of the 1.1-μm microspheres in $NaHCO_3$-buffered solution increased with transport distance before decreasing (Figure 5), as had been observed in experiments using MOPS as buffer (Figure 1), indicating that spatial variation of deposition rate coefficients occurred even under simple solution chemistries lacking organic matter. It is therefore possible that the observed profiles of Redman et al. (*9*, *10*) and Harter et al. (*18*) were not due to adsorbed organic matter on the sediment surfaces, but rather due to processes fundamental to filtration under unfavorable conditions. Equivalent results (hyper-exponential decreases) were obtained using MOPS and $NaHCO_3$ buffers for the 1.0-μm microspheres (0.001 M ionic strength) (Figure 3, bottom), further demonstrating that MOPS buffer was not the determinant of the profile shape.

Conditions Promoting Distance-Dependent Deposition. The discrepancies between the observed retained profiles versus those generated using a single deposition rate decreased with increasing ionic strength (Figures 1 and 5, bottom) and were eliminated under favorable deposition conditions (Figure 6), as was observed for the retained profiles in the glass beads (*17*). Favorable conditions were generated using amine-modified polystyrene latex microspheres (0.93 μm, Molecular Probes, Inc.). The influent concentration was

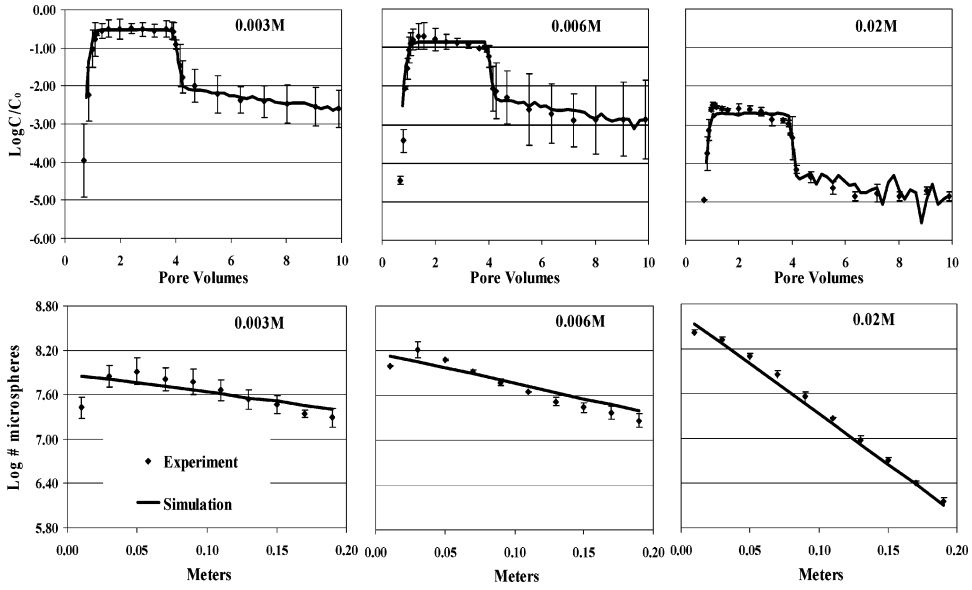

FIGURE 5. Effluent breakthrough−elution curves (top) and retained profiles (bottom) of the 1.1-μm microspheres at different ionic strengths using $NaHCO_3$ buffer (flow rate = 4 m day^{-1}). Error bars represent standard deviations in results from replicate experiments ($n \geq 2$). Solid lines represent simulations using the particle tracking model with a single deposition rate coefficient.

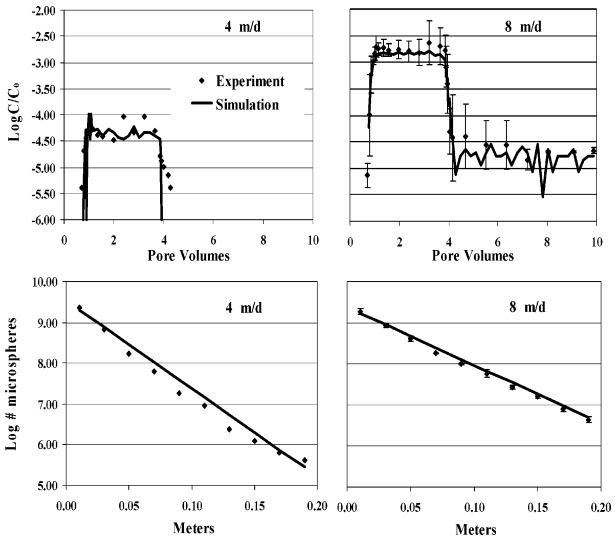

FIGURE 6. Effluent breakthrough−elution curves (top) and retained profiles (bottom) of amine-modified microspheres (0.93 μm) at flow rates of 4 m day^{-1} (left) and 8 m day^{-1} (right). Ionic strength = 0.001M for both flow rates. Error bars represent standard deviations in results from replicate experiments ($n \geq 2$). Solid lines represent simulations using the particle tracking model with a single deposition rate coefficient.

1.5×10^7 particles mL^{-1}, and the experiments were run with MOPS buffer at an ionic strength of 0.001 M and flow rates of 4 and 8 m day^{-1}. Higher influent concentrations were used to ensure reliable detection of effluent concentrations, which were expected to be very low due to lack of an energy barrier.

The effluent breakthrough curves and retained profiles of amine-modified microspheres were fit well simultaneously using a constant deposition rate coefficient (Figure 6), indicating that distance-invariant deposition rate coefficients are relevant only under favorable deposition conditions. The observed log-linear decrease in retained amine-modified microsphere concentrations with distance (Figure 6 bottom) argues against sediment and flow heterogeneities as sources of spatial variation in deposition rate coefficients under unfavorable conditions, because they would manifest regardless of favorable or unfavorable conditions.

The deposition rate coefficients for amine-modified microspheres (favorable conditions) increased from 8.5 to 10.8 h^{-1} with an increase in flow rate from 4 to 8 m day^{-1}. The same trend in deposition rate coefficient was observed in the glass beads (*17*), and the observed deposition rate coefficients in the glass beads were in quantitative agreement (within 10%) with the predictions based on filtration theory as described in Li et al. (*17*). In contrast, the deposition rate coefficients in quartz sand (Table 1) and glass beads (*17*) under unfavorable conditions (1.1-μm carboxylate-modified microspheres) decreased with increasing flow rate, suggesting an influence of hydrodynamic drag on the deposition process under unfavorable conditions. The deposition rate coefficient values in quartz sand were higher by a factor of about 2 than those determined in glass beads under equivalent favorable conditions (*17*), indicating that the roughness of the quartz sand enhanced deposition of the amine-modified microspheres.

Implications for Deposition under Unfavorable Conditions. The deviations of retained profiles from log-linear behavior were not produced by re-entrainment, or by adsorption of organic matter, or by artifacts arising from the quartz sand, because both hyper-exponential and non-monotonic deviations were observed on that sand for similarly sized microspheres. The deviations were present only under unfavorable deposition conditions and increased with increasingly unfavorable conditions. Hence, the colloid−surface interaction potential (e.g., energy barrier or secondary minimum) is strongly implicated to play a role in causing the observed deviations in the retained profiles. Unfortunately, the inability of theory to predict deposition under unfavorable conditions (*22*) severely limits the ability of DLVO-type analyses to enhance interpretation of the data presented here. The actual interaction energy profile within the first few nanometers is not known reliably (e.g., ref *23*). Despite these shortcomings, interaction energies between the 1.1-μm microspheres and the quartz sand were determined using DLVO theory. The zeta potentials of the microspheres (−67.6, −65.3, and −63.2 mV for 0.003, 0.006, 0.02 M, respectively) and crushed quartz sand (−92.5, −83.4, and −68.8 mV for 0.003, 0.006, 0.02 M, respectively) were measured using micro-electrophoresis (Zetaplus Analyzer,

Brookhaven Inc.). The electrostatic repulsive interaction was calculated on the basis of the linear superposition equation developed by Gregory (*24*). The retarded van der Waals attractive interaction was calculated on the basis of the approximate expressions developed also by Gregory (*25*). The decay length for the van der Waals interaction was 100 nm, and Hamaker constants were 6.8×10^{-21} and 4.2×10^{-21} J for microsphere−water−quartz and microsphere−water−microsphere systems, respectively. These Hamaker constants were obtained by combining the Hamaker constants of individual materials, 6.6×10^{-20} J of polystyrene (*26*), 3.7×10^{-20} of water (*26*), and 8.86×10^{-20} of quartz (*27*). The depths of the secondary minima were 0.2, 0.4, and 1.6 kT at 0.003, 0.006, and 0.02 M ionic strength in MOPS buffer, with corresponding separation distances of 70, 45, and 21 nm, respectively. The heights of the energy barrier were 4.2×10^3, 3.5×10^3, and 2.4×10^3 kT, respectively, at the above ionic strengths. These barriers would be expected to preclude deposition in the primary minimum, and the depths of the secondary minima are mostly small relative to the one-dimensional intrinsic energy of the colloids (0.5 kT). However, as stated above, the magnitudes of these characteristics of the energy profiles are insufficiently accurate under unfavorable conditions to allow a meaningful comparison to the experimental data.

Previous work has described the insensitivity of colloid deposition rates to ionic strength under unfavorable conditions, relative to expectations from theory (*22*). The porous media-based causes invoked to explain colloid deposition under unfavorable conditions, surface charge heterogeneity (*22*, *28*) and surface roughness (*22*, *29*) do not explain the retained profiles shown here, because these characteristics would have been homogeneously distributed within the repacked columns. The retained profiles shown here serve as another window into the intriguing issue of colloid deposition under unfavorable conditions, and combined with direct observation techniques they hold promise to reveal the processes governing deposition under unfavorable conditions.

Implications for Environmental Systems. The results presented here demonstrate that spatial variation of colloid deposition rate coefficients is ubiquitous under unfavorable conditions. Spatial variations in deposition rate coefficients were demonstrated to take monotonic and nonmonotonic forms depending on experimental conditions, although the latter form appears to be observed less commonly than the former. Whether other forms of retained profiles are possible has yet to be demonstrated. Most environmentally relevant groundwater conditions are unfavorable for deposition; that is, both colloids and sediments typically carry overall negative surface charge (*30*, *31*). Hence, it is expected that deviations from log-linear decreases in retained and mobile colloid concentrations from a source should be the norm in colloid transport in the subsurface environment. Given the sensitivity to experimental conditions of the form and extent of deviation from spatially constant deposition rates, current practices that utilize log-linear extrapolation of discreet measurements of colloid attenuation (e.g., estimation of well set-back distances from potential pathogen sources) cannot be considered reflective of actual changes in removal of colloids with distance from source and may need to be revised.

Acknowledgments

This work was funded by a grant from the National Science Foundation Hydrologic Sciences Program (EAR 0087522) to W.P.J. Any opinions, findings, and conclusions or recommendations expressed in this material are those of the author(s) and do not necessarily reflect the views of the National Science Foundation.

Literature Cited

(1) Yao, K. M.; Habibian, M. T.; O'Melia, C. R. Water and waste water filtration: Concepts and applications. *Environ. Sci. Technol.* **1971**, *5*, 1105−1112.
(2) Albinger, O.; Biesemeyer, B. K.; Arnold, R. G.; Logan, B. E. Effect of bacterial heterogeneity on adhesion to uniform collectors by monoclonal populations. *FEMS Microbiol. Lett.* **1994**, *124*, 321−326.
(3) Baygents, J. C.; Glynn, J. R., Jr.; Albinger, O.; Biesemeyer, B. K.; Ogden, K. L.; Arnold, R. G. Variation of surface charge density in monoclonal bacterial populations: implications for transport through porous media. *Environ. Sci. Technol.* **1998**, *32*, 1596−1603.
(4) Simoni, S. F.; Harms, H.; Bosma, T. N. P.; Zehnder, A. J. B. Population heterogeneity affects transport of bacteria through sand columns at low flow rates. *Environ. Sci. Technol.* **1998**, *32*, 2100−2105.
(5) Bolster, C. H.; Mills, A. L.; Hornberger, G.; Herman, J. Spatial distribution of deposited bacteria following miscible displacement experiments in intact cores. *Water Resour. Res.* **1999**, *35*, 1797−1807.
(6) Harvey, R. W.; Garabedian, S. P. Use of colloid filtration theory in modeling movement of bacteria through a contaminated sandy aquifer. *Environ. Sci. Technol.* **1991**, *25*, 178−185.
(7) Deflaun, M. F.; Murray, C. J.; Holben, M.; Scheibe, T.; Mills, A.; Ginn, T.; Griffin, T.; Majer, E.; Wilson, J. L. Preliminary observations on bacterial transport in a coastal plain aquifer. *FEMS Microbiol. Rev.* **1997**, *20*, 473−487.
(8) Zhang, P.; Johnson, W. P.; Scheibe, T. D.; Choi, K.; Dobbs, F. C.; Mailloux, B. J. Extended tailing of bacteria following breakthrough at the Narrow Channel Focus Area, Oyster, Virginia. *Water Resour. Res.* **2001**, *37*, 2687−2698.
(9) Redman, J. A.; Grant, S. B.; Olson, T. M.; Estes, M. K. Pathogen filtration, heterogeneity, and the potable reuse of wastewater. *Environ. Sci. Technol.* **2001**, *35*, 1798−1805.
(10) Redman, J. A.; Estes, M. K.; Grant, S. B. Resolving macroscale and microscale heterogeneity in pathogen filtration. *Colloids Surf., A* **2001**, *191*, 57−70.
(11) Bales, R. C.; Li, S. M.; Yeh, T. C. J.; Lenczewski, M. E.; Gerba, C. P. Bacteriophage and microsphere transport in saturated porous media: forced-gradient experiment at Borden, Ontario. *Water Resour. Res.* **1997**, *33*, 639−648.
(12) Pieper, A. P.; Ryan, J. N.; Harvey, R. W.; Amy, G. L.; Illangasekare, T. H.; Metge, D. W. Transport and recovery of bacteriophage PRD1 in a sand and gravel aquifer: effect of sewage-derived organic matter. *Environ. Sci. Technol.* **1997**, *31*, 1163−1170.
(13) Schijven, J. F.; Hoogenboezem, W.; Hassanizadeh, S. M.; Peters, J. H. Modeling removal of bacteriophages MS2 and PRD1 by dune recharge at Castricum, Netherlands. *Water Resour. Res.* **1999**, *35*, 1101−1111.
(14) Woessner, W. W.; Ball, P. N.; DeBorde, D. C. Troy, T. L. Viral transport in a sand and gravel aquifer under field pumping conditions. *Ground Water* **2001**, *36*, 886−894.
(15) Bolster, C. H.; Mills, A. L.; Hornberger, G.; Herman, J. Effect of intra-population variability on the long-distance transport of bacteria. *Ground Water* **2000**, *38*, 370−375.
(16) Tufenkji, N.; Redman, J. A.; Elimelech, M. Interpreting deposition patterns of microbial particles in laboratory-scale column experiments. *Environ. Sci. Technol.* **2003**, *37*, 616−623.
(17) Li, X.; Scheibe, T. D.; Johnson, W. P. Apparent decreases in colloid deposition rate coefficient with distance of transport under unfavorable deposition conditions: a general phenomenon. *Environ. Sci. Technol.* **2004**, *38*, 5616−5625.
(18) Harter, T.; Wagner, S.; Atwill, E. R. Colloid transport and filtration of cryptosporidium parvum in sandy soils and aquifer sediments. *Environ. Sci. Technol.* **2000**, *34*, 62−70.
(19) Tong, M.; Li, X.; Brow, C.; Johnson. W. P. Detachment-influenced transport of an adhesion-deficient bacterial strain within water-reactive porous media. *Environ. Sci. Technol.*, in press.
(20) Li, X.; Zhang, P.; Lin, C. L.; Johnson, W. P. Role of hydrodynamic drag on microsphere deposition and re-entrainment in porous media under unfavorable conditions. *Environ. Sci. Technol.*, in press.
(21) Meinders, J. M.; Busscher, H. J. Influence of interparticle interactions on blocked areas and desorption during particle deposition to glass in a parallel plate flow chamber. *Langmuir* **1995**, *11*, 327−333.
(22) Elimelech, M.; O'Melia, C. R. Kinetics of deposition of colloidal particles in porous media. *Environ. Sci. Technol.* **1990**, *24*, 1528−1536.
(23) Hahn, M. W.; O'Melia, C. R. Deposition and reentrainment of Brownian particles in porous media under unfavorable chemical

conditions: some concepts and applications. *Environ. Sci. Technol.* **2004**, *38*, 210−220.
(24) Gregory, J. Interaction of unequal double layers at constant charge. *J. Colloid Interface Sci.* **1975**, *51*, 44−51.
(25) Gregory, J. Approximate expressions for retarded van der Waals interaction. *J. Colloid Interface Sci.* **1981**, *83*, 138−145.
(26) Israelachvili, J. N. *Intermolecular and surface forces*, 2nd ed.; Academic Press: London, 1992.
(27) Bergstrom, L. Hamaker constants of inorganic materials. *Adv. Colloid Interface Sci.* **1997**, *70*, 125−169.
(28) Johnson, P. R.; Sun, N.; Elimelech, M. Colloid transport in geochemically heterogeneous porous media: modeling and measurements. *Environ. Sci. Technol.* **1996**, *30*, 3284−3293.
(29) Shellenberger, K.; Logan, B. E. Effect of molecular scale roughness of glass beads on colloidal and bacterial deposition. *Environ. Sci. Technol.* **2002**, *36*, 184−189.
(30) Davis, J. A. Adsorption of natural dissolved organic matter at the oxide/water interface. *Geochim. Cosmochim. Acta* **1982**, *46*, 2381−2393.
(31) Tipping, E.; Cooke, D. The effects of adsorbed humic substances on the surface charge of goethite (α-FeOOH) in freshwaters. *Geochim. Cosmochim. Acta* **1982**, *46*, 75−80.

Received for review July 7, 2004. Revised manuscript received December 3, 2004. Accepted December 9, 2004.

ES048963B